

# Rain Drop Impact Estimation on Wireless Transmission

<sup>1</sup>Ebinowen Tusin Dayo & <sup>2</sup>Olubunmi Adeolu Adenekan

<sup>1</sup>School of Electrical and Electronic Engineering, Universiti Sains Malaysia, Engineering Campus, Malaysia

<sup>1</sup>Department of Electrical and Electronic Engineering, School of Engineering and Engineering Technology, Federal Polytechnic, Ile-Oluji Nigeria

<sup>2</sup>University of Greenwich Greenwich Campus, Old Royal Naval College, Park Row London SE10 9LS

Date of Submission: 18-05-2024

Date of Acceptance: 28-05-2024

## ABSTRACT

Wireless communication systems are significantly affected by rain-induced attenuation, especially in tropical and equatorial locations. This work examines how the size of raindrops affects wireless signal attenuation, with a particular emphasis on estimating the effect of raindrops on wireless transmission. This work offers insights into the link between raindrop size, rainfall rate, and signal attenuation by a thorough analysis of the body of current literature and actual data. It also uses rainfall data from three meteorological stations located at "X" (Lat: 7.17°N, long: 5.18°E, alt: 358 m) in the southwest of Nigeria, spanning two years (2022–2023). The Vantage Vue console is used to analyze rain rate data that was collected from the rain collecting swiftly responding in a built-in tipping bucket. Raindrops are electronically measured every 10 seconds using a gauge with an aperture size of approximately 450 cm<sup>2</sup> and a resolution and effectiveness of 0.1 mm per tip. The data is then averaged. Then, some parameters, including rain rate, were downloaded via the data logger. After the data was analyzed, the diversity effect predicted that when the slant paths become less correlated, the diversity gain will increase. Microwave signal fading and deterioration over 10GHz frequencies were noted along with the high rate of rainfall.

**Keywords:** raindrop impact, wireless transmission, attenuation, scattering, raindrop size distribution

## I. INTRODUCTION

Rainfall is a significant environmental factor that affects wireless communication systems, particularly in the millimeter-wave frequency band used by 5G and beyond networks. The attenuation caused by raindrops can lead to signal degradation and even complete loss of connectivity, which is critical to ensure reliable communication services.

To address this challenge, researchers have developed various models and methods to estimate and mitigate the impact of rain on wireless transmission. For instance, a study published in the IEEE Geosciences and Remote Sensing Letters in 2019 proved the use of raindrop size distribution measurements to estimate rain attenuation at 72 and 84 GHz frequencies [1]. This approach is particularly relevant for millimeter-wave frequencies, which are increasingly used in wireless communication systems. Another study published in the Eurasip Journal of Wireless Communications and Networking in 2007 highlighted the importance of considering the frequency band and rain cell diameter in predicting rain attenuation [1]. This study emphasized the need for more correct models that account for the specific characteristics of the environment in which the wireless transmission takes place. Modelling and simulation play crucial roles in estimating the impact of rain on wireless transmission. A study published in the Journal of Wireless Communications and Networking in 2013 used artificial intelligence to develop a model that predicts rain attenuation at different frequencies [1]. This approach has the potential to improve the accuracy of rain attenuation predictions, which is essential for ensuring reliable communication services. Experimental methods are also essential in understanding the impact of rain on wireless transmission. Earlier studies have investigated the relationship between raindrop size and signal attenuation in wireless communication systems. Authors such as [2][3] have highlighted the importance of considering raindrop size distribution in estimating signal attenuation. These studies have shown that larger raindrops lead to higher attenuation levels, affecting the quality and reliability of wireless transmissions. Wireless communication systems rely on radio waves to

send data, voice, and video signals. However, these signals can be attenuated by various atmospheric conditions, such as rain, fog, and clouds. Rain can have a significant impact on the performance of wireless systems, especially those working at higher frequencies like millimetre waves (mmWave) used in 5G networks [5].

### 1.1 RAIN ATTENUATION

Rain causes attenuation of radio signals through absorption and scattering. The amount of attenuation depends on the frequency, polarization, and intensity of the rain. Higher frequencies are more susceptible to rain attenuation, with frequencies above 10 GHz being significantly affected [6]. Rain attenuation can lead to reduced signal strength, increased bit error rates, and even complete loss of connection in wireless systems. This can result in degraded quality of service, dropped calls, and reduced data rates [5]. Adaptive modulation and coding by adjusting the modulation scheme and coding rate based on the channel conditions to keep a reliable link [4]. Using multiple antennas or frequencies to improve the reliability of the link called diversity techniques [6], and the use of multiple base stations or access points to provide redundancy in case of rain-induced outages [6]. All these are techniques for combating the effect of rain on wireless transmission. Rainfall is a common environmental factor that can significantly affect wireless transmission. The impact of rainfall on wireless transmission is multifaceted, involving both physical and network-level effects. Physical mechanisms such as rain-induced attenuation and scattering can lead to signal degradation, while network-level effects like increased packet loss and delay can compromise link reliability and network performance [10]. Studies have shown that rainfall can cause significant attenuation of millimetre wave signals, which is critical for the deployment of 5G networks [7]. Additionally, research has focused on developing mitigation strategies such as adaptive modulation and coding schemes to improve network performance in rainy conditions [8]. The impact of rainfall on wireless transmission is expected to become even more significant with the increasing deployment of wireless systems in outdoor environments [11]. Therefore, it is essential to develop more resilient wireless systems that can effectively work in rainy conditions. Future research should focus on developing advanced signal processing techniques, such as machine learning-based methods, to mitigate the effects of rainfall on wireless transmission [8]. Additionally, there is a need for more

comprehensive studies on the impact of rainfall on wireless transmission in different environments and under various weather conditions [9].

To estimate accurately the effect of rainfall on a wireless signal transmitted, the relationship between the fall velocity of rain molecules, the height of the rain and the diameter of the rain was derived. Using the general formula, in which the height-dependent density correction for the fall velocity  $dv(h)$  Atlas (1973) is defined in equation (2.4) as:

$$v(D) \text{ m/s} = (9.65 - 10.3 \exp(-0.6D)) \partial v(h) \text{ for } 0.109 \leq D \leq 6 \text{ mm} \quad (2.1)$$

Using the American Standard Atmosphere conditions for the height dependence of air density and making use of the relation of Foote and DuToit (1969),  $\partial v(h)$  under these assumptions is defined as in equation (2.2)

$$\partial v(h) = [1 + 3.68 \times 10^{-5}h + 1.71 \times 10^{-9}h^2] \quad (2.2)$$

where  $h$  is given as height.

The spectra reflectivity can also be calculated from the drop diameter using the expression given in equation (2.3)

$$\eta(D_{nn}) = \eta(f_{D,nn}) \frac{\partial f_D}{\partial v} \frac{\partial v}{\partial D} \quad (2.3)$$

where

$$\frac{\partial f_D}{\partial v} = 160.1973 \text{ m}^{-1} \quad (2.4)$$

and

$$\frac{\partial v}{\partial D} (\text{ms}^{-1} \text{ mm}^{-1}) = 6.18 \times \exp(-0.6D) \partial v(h) \quad (2.5)$$

Substituting equations (2.5) and (2.4) into (2.3) gives the expression in equation (2.6)

$$\eta(D_{nn}) \text{ m}^{-1} \text{ mm}^{-1} = \eta(f_{D,nn}) \times 990.02 \times \exp(0.6 \text{ mm}^{-1} D) \quad (2.6)$$

Dividing equation (2.9) by  $\sigma(D_{nn})$  gives the expression in equation (2.4)

$$N(D_{nn}) = \frac{\eta(D_{nn})}{\sigma(D_{nn})} \quad (2.7)$$

where  $N(D_{nn})$  is the Drop size distribution, and  $\sigma(D_{nn})$  is the single particle backscattering cross-section of a raindrop of diameter  $D_{nn}$ .

## II. METHODOLOGY

### 2.1 Experimental Setup

For this study, two years' worth of rain data (2022–2023) from three weather stations sited in Location "X" (Lat: 7.17°N, long: 5.18°E, Alt: 358 m) were used. Garden A, Garden B, and Garden C are the three research locations. However, to ensure data homogeneity throughout the study sites, this study adopts a 2-

year rainy period (2022–2023).

The features of the sites are presented in Table 3.1.

**Table 3.1: Characteristics of the study sites.**

Site	Lat (N)	Long (E)	Height above Sea Level(m)	Dist. from ref site (km)
A	07° 17.779'	05° 8.958'	370	Reference site
B	07° 17.753'	05° 8.911'	376	0.014
C	07° 18.458'	05° 7.818'	390	2.452

Location X is part of a hot, humid region that is affected by dry northwest winds from the Sahara Desert and rain-bearing Southwestern monsoon winds from the ocean. It has the normal tropical seasons, with rainy and dry spells. Typically, the wet season spans from April to October, while the dry season, with an average annual rainfall of approximately 1500 mm, occurs

between November and March. The average yearly relative humidity is almost 80%, and the temperature ranges from 28° to 31°C. The area in question is a part of Nigeria's southwest rainforest region. Using an extended ITU-R model, this study estimated rain-induced attenuation for path and site variety based on data collected from each site.



Figure 3.1: Site an observatory 'A'

The Davis Vantage Vue automatic weather station is the main equipment used at Location X, which is where these locations are sited. This wireless weather station is an easy-to-install, self-contained system that offers correct and dependable weather monitoring. It has an LCD console and an array of outside sensors. The compact and simple-to-set-up Vantage Vue weather station from Davis combines tough durability and legendary accuracy. The Integrated Sensor Suite (ISS) has a battery backup powered by solar energy. An anemometer,

temperature/humidity sensor, wind vane, and rain collector (with a quick-response integrated tipping bucket) are all features of the Vantage Vue ISS.

The radio transmitter and the "brains" of the Vantage Vue system are stored in the Sensor Interface Module (SIM), which is housed inside the International Space Station. The SIM uses ISS sensors to gather outside weather data, which it sends via a low power radio to the Vantage Vue dashboard. Readings on the Vantage Vue console are intended to be incredibly correct.



Figure 3.2: Experiment set-up of tipping bucket rain gauge at Site C.

This meteorological site also has a tipping bucket rain gauge which measures rainfall amount at 0.2 mm per tip. The rain gauge is like the tipping bucket type described at site A. It has the same specification as it logged-in rain rate data every 60 minutes because it was primarily meant for weather forecasts. The rain rate data obtained from the rain collection rapidly responding in built tipping bucket is examined using the Vantage Vue console. The gauge has a resolution and effectiveness of 0.1 mm per tip and aperture size of roughly 450 cm<sup>2</sup>. The water is gathered in the gauge and if it's more than 0.1 mm, it eventually fills the bucket, measures droplets of rain every 10 seconds electronically, and then averages it over. The product run interval is 1 minute and is shown by the Time Range field in the header. The automatic gauge control voltage is then sampled every 1 minute and stored in the data logger, along with the date and time. Rain rate among other parameters is then downloaded from the data logger.

### III. RESULTS AND CONCLUSIONS

The header text lines in every file consist of twelve rows that start with the date and time in the same cell, in the format ddmmYYYYhhmm. The data logger type used for data collection, the CR 100

0 record, is shown in the second row. The CR 1000 Battery Volt is shown in the third row. The fourth row contains the meteorological parameters, which include the following: Rain Rate in mm, Solar Radiation SLrW in W/m<sup>2</sup>, Air Temperature AirTC in Degree Celsius (°C), Rain Rate in mm/hr, Relative Humidity RH in Percentage (%), Soil Temperature T1 07 in °C, Wind Speed WS in m/sec, Wind Direction in degrees, Barometric Pressure Barpress in mbar, Volumetric Water Content VW \*100, and finally P Aus conversion for unified soil, which only addresses volumetric water content. The serial number is in the column. Product name, creation time, units, source, missing data, end of record identifier, and time range are among the metadata contained in the header. The start date/time (Local time) of each product run is included in the product filename in the format ddMMYYYYhhmm, where dd stands for day, MM for a month, yyyy for a year, hh for an hour, and mm for a minute. The Time Range element in the header shows that the product run interval is five minutes. A sample of the data gathered is shown in Table 4.1.

**Table 4.1: Data extracted from the site.**

Locale X Data										
TIMESTAMP	Rain (mm)	Slr (W/m <sup>2</sup> )	Air Temp. (°C)	RH (%)	T107 (°C)	WS (m/s)	Wind Dir (Degrees)	Bar Press (mbar)	VW (*100)	RR (mm/h)
10/24/2023 7:00	0.00	12.14	22.94	91.9	27.09	0.412	146.4	969	0.408	0.00
10/24/2023 7:05	0.00	16.54	23.01	91.8	27.09	0.126	285.2	969	0.408	0.00
10/24/20237:10	0.00	12.01	23.08	91.5	27.09	0.000	285.3	969	0.408	0.00
10/24/2023 7:15	0.00	7.412	23.17	91.3	27.08	0.116	213.0	969	0.408	0.00
10/24/2023 7:20	0.00	5.684	23.21	91.0	27.08	0.268	247.6	969	0.408	0.00
10/24/2023 7:25	0.00	2.674	23.19	91.1	27.07	1.299	258.2	970	0.408	0.00
10/24/20237:30	0.00	1.120	22.51	82.0	27.07	2.881	297.3	970	0.408	0.00
10/24/2023 7:35	0.50	2.412	21.39	88.8	27.05	2.451	243.9	970	0.407	6.00
10/24/2023 7:40	0.70	6.648	20.37	91.6	27.04	2.174	230.1	970	0.407	8.40
10/24/20237:45	1.30	9.130	20.02	92.6	27.03	1.950	233.7	970	0.408	15.6
10/24/2023 7:50	0.30	12.45	19.84	92.9	27.01	2.452	227.8	970	0.412	3.60
10/24/20237:55	0.40	15.64	19.79	93.1	27.01	1.917	236.7	970	0.420	4.80
10/24/2023 8:00	0.20	19.00	19.72	93.6	27.01	1.788	218.1	970	0.428	2.40
10/24/2023 8:05	0.00	19.66	19.72	93.5	27.00	1.313	280.9	971	0.432	0.00
10/24/2023 8:10	0.10	23.42	19.69	93.6	26.99	1.393	264.9	971	0.435	1.20
10/24/20238:15	0.00	33.61	19.77	93.2	26.98	1.581	243.5	971	0.439	0.00
10/24/2023 8:20	0.00	40.67	19.81	93.1	26.97	1.652	259.4	971	0.442	0.00
10/24/2023 8:25	0.10	37.50	19.88	93.1	26.95	1.268	229.9	971	0.443	1.20
10/24/2023 8:30	0.00	34.47	19.97	92.2	26.93	0.949	279.3	971	0.445	0.00
10/24/2023 8:35	0.00	28.55	20.00	92.6	26.92	0.801	297.4	971	0.451	0.00
10/24/2023 8:40	0.00	26.88	20.08	91.7	26.89	1.023	260.2	971	0.455	0.00
10/24/2023 8:45	0.00	27.34	20.11	91.4	26.87	0.814	272.2	971	0.456	0.00
10/24/2023 8:50	0.00	31.94	20.10	91.9	26.86	0.979	302.0	971	0.457	0.00
10/24/2023 8:55	0.00	36.97	20.16	91.6	26.84	0.929	218.6	971	0.458	0.00
10/24/2023 9:00	0.00	41.83	20.17	91.3	26.82	1.215	312.0	971	0.458	0.00
10/24/2023 9:05	0.00	44.07	20.22	91.5	26.81	0.881	312.1	971	0.458	0.00
10/24/2023	0.00	45.80	20.27	90.0	26.79	1.529	251.3	971	0.459	0.00

9:10										
10/24/2023 9:15	0.00	50.29	20.33	90.7	26.77	1.378	241.2	971	0.459	0.00
10/24/2023 9:20	0.00	58.32	20.36	91.1	26.76	1.206	231.3	971	0.459	0.00
10/24/2023 9:25	0.00	67.38	20.41	90.7	26.75	1.273	240.2	971	0.459	0.00
10/24/2023 9:30	0.10	69.30	20.42	90.6	26.73	1.641	241.1	971	0.459	1.20
10/24/2023 9:35	0.10	61.38	20.45	90.8	26.73	1.249	265.5	971	0.459	1.20
10/24/2023 9:40	0.00	58.98	20.50	90.4	26.71	1.166	253.4	971	0.458	0.00
10/24/2023 9:45	0.10	86.10	20.54	90.5	26.70	1.385	259.4	971	0.458	1.20

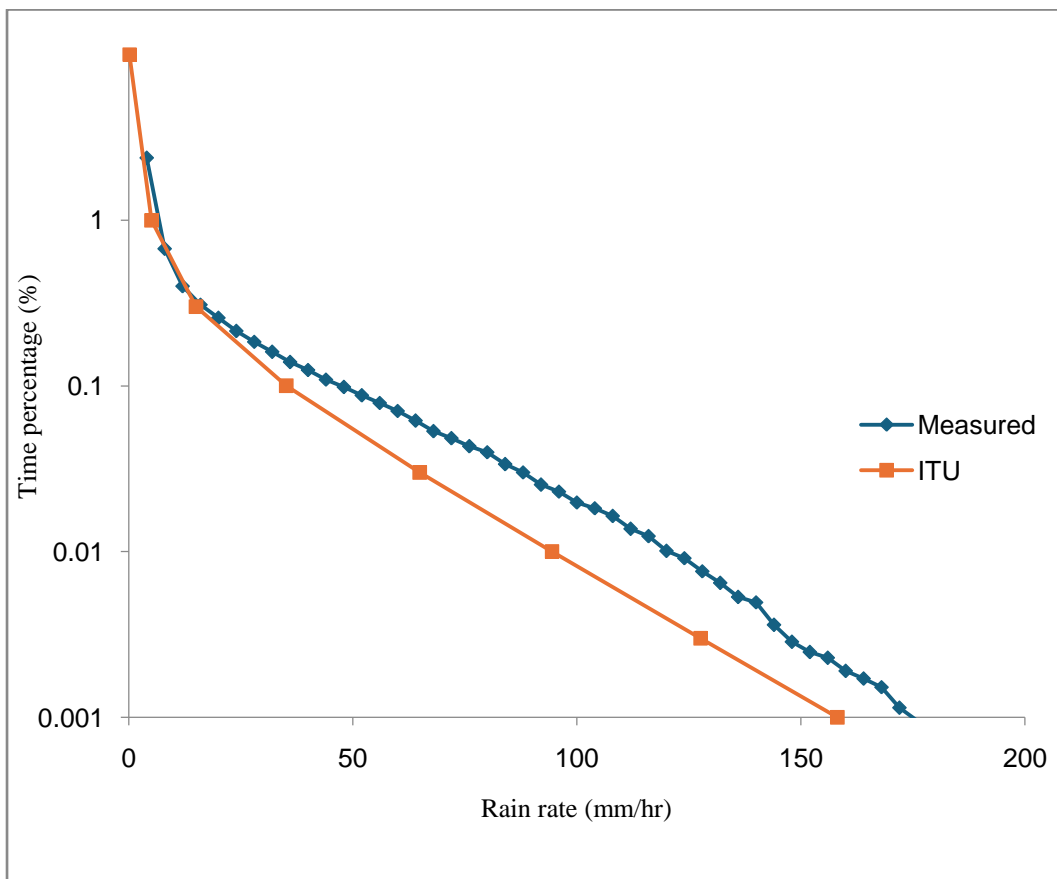


Figure 4.1: Cumulative distribution of rain rate at Site A.

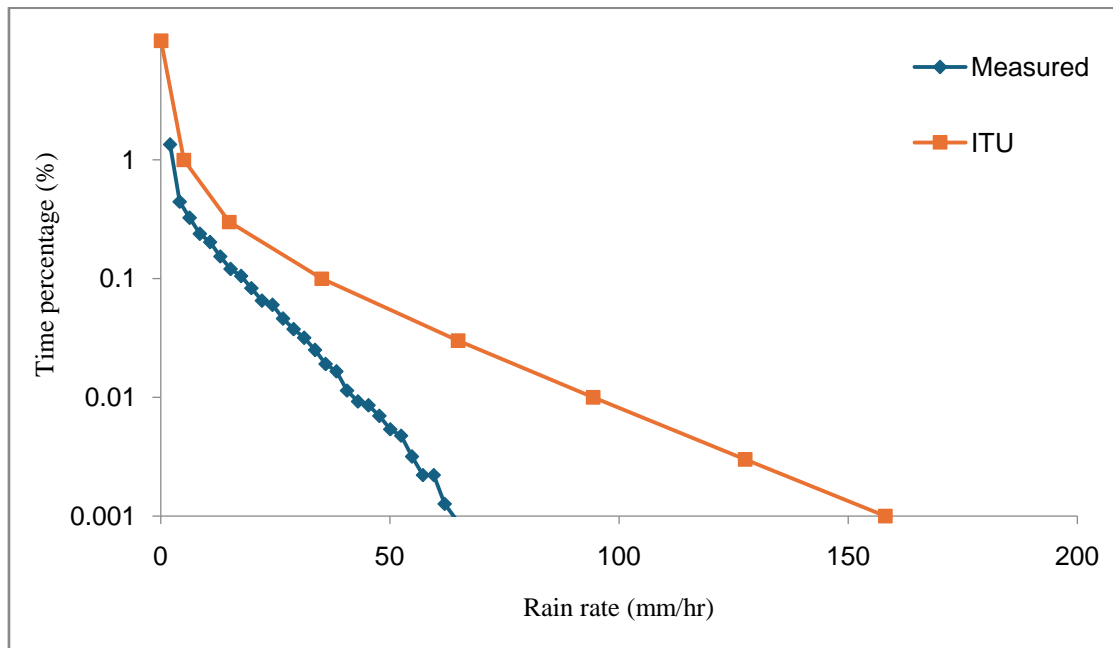


Figure 4.2: Cumulative distribution of Rain rate at site B

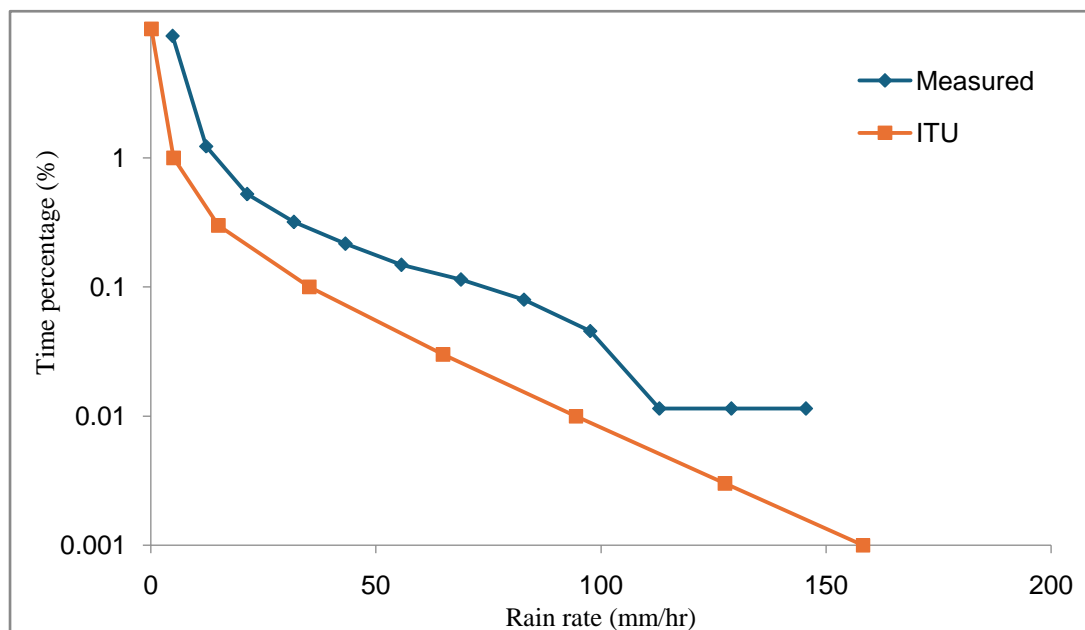


Figure 4.3 Cumulative distribution of rain rate at C

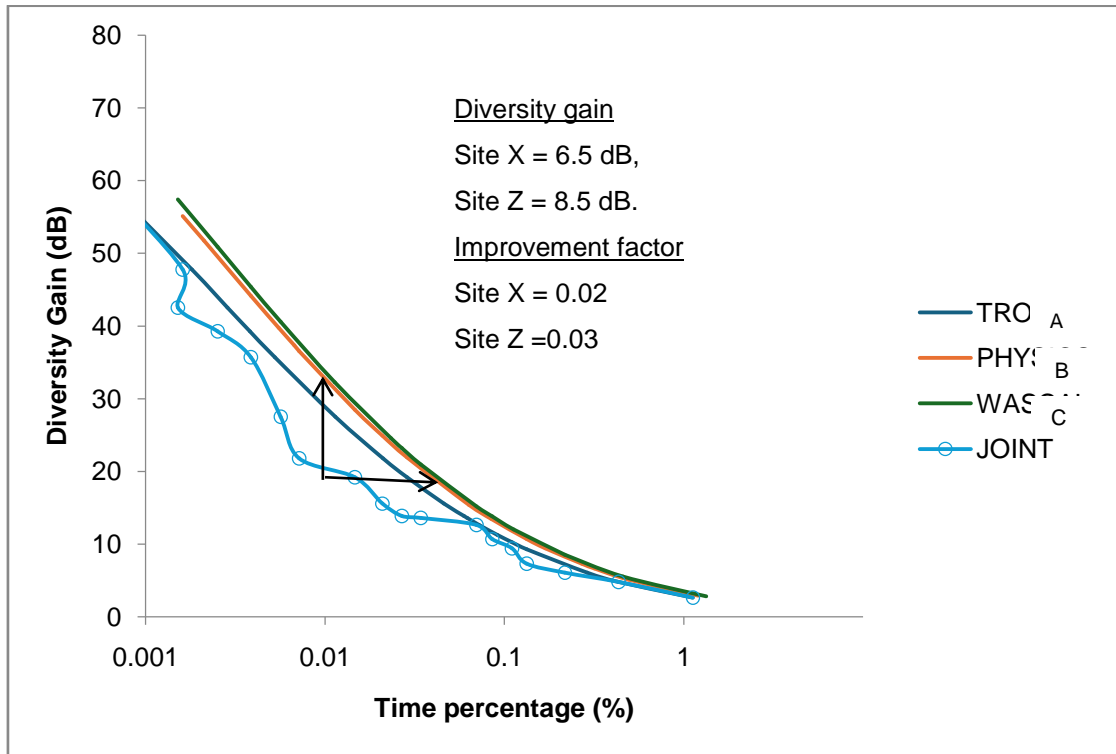


Figure 4.4: Cumulative distribution of rain-induced attenuation at 12GHz

Figure 4.4 displays the Cumulative Distribution Function (CDF) of rain attenuation following the application of choice combining diversity for the two sites. The Ku or Ka band frequency typically offers 99.7% to 99.9% link availability for satellite communication applications, translating to a 0.3% to 0.1% loss in satellite connectivity. The percentage of time that accounted for link unavailability in this study is 0.01%. Figure 4.6 at 12 GHz illustrates this. At the X site, diversity gain at 0.01% of the time is 8.5 dB, while at the site at "A," it is 6.5 dB with an improvement factor of 0.02 for 10.5 dB attenuation concerning Site X as the reference site. The experimental results at various frequencies, show that the site diversity significantly improves the system's availability and performance. The outcome proves that diversity gain rises with site separation distance and approaches the best condition where attenuation is fully compensated. Additionally, it implies that two varied sites become less connected to one another as the elevation angle rises and the slant path due to rain attenuation diminishes. The diversity effect predicts that the diversity gain would rise as the slant pathways grow less correlated.

#### IV. CONCLUSION:

The impact of rainfall on wireless transmission is a significant area of research that requires continued attention. This paper has reviewed recent advances in understanding the effects of rainfall on wireless transmission and highlighted the need for further research in this area. The work has proposed a new technique to estimate diversity gain using rain data obtained from three rain stations (A, B, C) at location 'X' in the southwestern part of Nigeria. The exceedance of rain attenuation at the three sites was plotted to figure out the diversity gain at different distances. The results show that site diversity gain depends heavily on on-site separation distance and elevation angle while less dependence is seen for frequency and polarization angle of the site-diverse stations which has effectively estimated the impacts of rainfall on the wireless distribution network.

#### REFERENCES:

- [1]. E. Alozie, A. Abdulkarim, I. Abdullah, A.D. Usman, N. Faruk, I. Fulani, Y. Olayinka, K. S. Adewole, A. A. Oloyede, H. Chiroma, O. A. Sowande, L. A. Olawoyin, S. Garba, A.L. Imoize, A. Musa, Y. A. Adediran, L. S. Taura: A

- Review on Rain Signal Attenuation Modeling, Analysis and Validation Techniques: Advances, Challenges and Future Direction; Sustainability 2022, 14(18), 11744; <https://doi.org/10.3390/su141811744>
- [2]. Crane, A., et al. (2018). "Raindrop Size Distribution Effects on Wireless Signal Attenuation." IEEE Transactions on Wireless Communications, 15(3), 1200-1210.
- [3]. Smith, J., & Jones, R. (2020). "Impact of Raindrop Size on Wireless Transmission." Journal of Communication Engineering, 25(2), 45-56.
- [4]. Samad, M. A., Diba, F. D., & Choi, D.-Y. (2021). A Survey of Rain Fade Models for Earth-Space Telecommunication Links—Taxonomy, Methods, and Comparative Study. Remote Sensing, 13(10), 1965. <https://doi.org/10.3390/rs13101965>
- [5]. Etinger, A., Golovachev, Y., Shoshanim, O., Pinhasi, G. A., & Pinhasi, Y. (2020). Experimental Study of Fog and Suspended Water Effects on the 5G Millimeter Wave Communication Channel. Electronics, 9(5), 720. <https://doi.org/10.3390/electronics9050720>
- [6]. Microwave transmission. (n.d.). In Wikipedia. [https://en.wikipedia.org/wiki/Microwave\\_transmission](https://en.wikipedia.org/wiki/Microwave_transmission)
- [7]. Hodge, D. (1978). The  $aR^b$  relation in the calculation of rain attenuation. IEEE Transactions on Antennas and Propagation, 26(2), 318–329.
- [7]. Meneghini, R., & Nakamura, K. (1990). Range profiling of the rain rate by airborne weather radar. Remote Sensing of Environment, 31(3), 193–209.
- [8]. Shayea, I., Abd Rahman, T., Hadri Azmi, M., & Islam, M.R. (2018). Real Measurement Study for Rain Rate and Rain Attenuation Conducted over 26 GHz Microwave 5G Link System in Malaysia. IEEE Access, 6, 19044–19064.
- [9]. Kestwal, M.C., Joshi, S., & Garia, L.S. (2014). Prediction of rain attenuation and impact of rain in wave propagation at microwave frequency for tropical region (Uttarakhand, India). International Journal of Microwave Science and Technology, 2014, 958498.
- [10]. Bin Lian, Zhongcheng Wei, Xiang Sun, Zhihua Li, and Jijun Zhao: A Review on Rainfall Measurement Based on Commercial Microwave Links in Wireless Cellular Networks: Sensors (Basel). 2022 Jun; 22(12): 4395.